

Invited Paper

Simulation Study of Electron Scattering in Crystalline Solid by Using Bohmian Quantum Trajectory Method

R.G. Zeng and Z.J. Ding*

Hefei National Laboratory for Physical Sciences at Microscale and Department of Physics, University of Science and Technology of China, Hefei, Anhui 230026, China

*zjding@ustc.edu.cn

(Received : November 3, 2010 ; Accepted : January 15, 2011)

Based on Bohmian quantum trajectory theory, an investigation of electron scattering in a thin crystal has been performed. A time-independent interaction potential was employed to describe electron scattering from model crystal. Quantum trajectories were calculated by a numerical solution of the time-dependent Schrödinger equation. The probability density functions and quantum trajectories representing the electron diffraction in real space were obtained from the calculation. The quantum trajectories provide an intuitive dynamics of the interaction process during the electron diffraction.

1. Introduction

Techniques with electron spectroscopy, diffraction and microscopy have played an important role in many fields for materials analysis. Among them many are based on electron diffraction phenomena, such as low energy electron diffraction [1], transmission electron diffraction [2], electron backscatter diffraction [3], Auger electron diffraction and photoelectron diffraction. Analysis of the measured data generally requires the understanding of electron-solid interaction process. Monte Carlo method has been widely used to study the electron-solid interaction for amorphous and polycrystalline solid with great success for electron spectroscopic study [4-6]. However such a Monte Carlo simulation of electron trajectory is basically a classical method, with which the crystal structural information and the electron coherent scattering are hardly to be taken into account. On the other hand, the quantum mechanical methods, such as multislice method, based on wave nature description of particle for coherent elastic scattering have been successful to derive diffraction effects. The classical non-coherent and quantum mechanical methods have their own advantages and disadvantages. The difficulty to combine both natures of particle and wave in theoretical investigation of electron interaction with crystalline solid comes from

the wave-particle duality. The single electron buildup of an interference pattern experiment [7] has clearly demonstrated the particle trajectory character with probability wave motion behavior of electrons. An alternative theoretical description is therefore expected to represent the wave-particle duality nature of microscopic particle, while offer a physical picture of diffraction phenomena in term of the well defined trajectories of microscopic particle. Such formalism for simulation of electron-matter interaction is able to be established based on the Bohmian quantum trajectory theory.

The quantum trajectory theory was firstly proposed by de Broglie [8] in 1927 and then developed by Bohm [9,10]. The basis of this theory is the standard quantum mechanics, while the concept of particle is introduced into the quantal description of nature [9]. The theory not only accounts for the quantum phenomena accurately but also provides an intuitive interpretation of interference according to particle trajectory. The theory has been recently applied to several physical and chemical problems. Philippidis et al. [11] have simulated the electron double-slit experiment and Sanz et al. have studied the atom-surface scattering to reinterpret the atom diffraction patterns [12] and the rainbow effect [13]. The objective of the current work is to study the dynamical process of electron diffraction in solid. The

time dependent wave function was obtained by numerically solving the time-dependent Schrödinger equation for a model thin crystal, and then the dynamic process of electron trajectory in diffraction is demonstrated.

2. Theory

The Bohmian quantum trajectory method [9,10,14] considers that the wave function represents an objectively real field. Besides the field, there is a particle (Bohmian particle) represented mathematically by a set of trajectories, which are always well defined and vary in a definite way. In order to obtain the equation of motion of the Bohmian particle, firstly the wave function is rewritten in a polar form $\psi = R \exp(iS/\hbar)$, where R and S are real representing the amplitude and phase, respectively. Inserting the wave function into the time-dependent Schrödinger equation (TDSE):

$$i\hbar \frac{\partial \psi(\mathbf{r}, t)}{\partial t} = -\frac{\hbar^2}{2m} \nabla^2 \psi(\mathbf{r}, t) + V(\mathbf{r}, t) \psi(\mathbf{r}, t), \quad (1)$$

and then by separating the equation into real and imaginary parts one can obtain two associated equations:

$$\frac{\partial S}{\partial t} = \frac{(\nabla S)^2}{2m} + V(\mathbf{r}) - \frac{\hbar^2}{2m} \frac{\nabla^2 R}{R}, \quad (2)$$

$$\frac{\partial R^2}{\partial t} + \nabla \left(\frac{R^2 \nabla S}{m} \right) = 0. \quad (3)$$

Eq. (2) is referred to quantum Hamilton-Jacobi (HJ) equation. The quantum HJ equation differs from the classical HJ equation by the addition of the so-called quantum potential term, $Q \equiv \hbar^2 \nabla^2 R / (2mR)$. The quantum potential is due to internal quantum forces. As in the classical HJ theory, the velocity field for Bohmian particle is defined as,

$$\mathbf{v} = \frac{\nabla S(\mathbf{r}, t)}{m} = \frac{\hbar}{m} \text{Im} \frac{\nabla \psi(\mathbf{r}, t)}{\psi(\mathbf{r}, t)}. \quad (4)$$

The quantum trajectory of the Bohmian particle associated to a given quantum state can thus be obtained by integrating the velocity field as,

$$\mathbf{r}(t) = \mathbf{r}_0(t_0) + \int_{t_0}^t (\nabla S/m) dt. \quad (5)$$

Eq. (3) is referred to continuity equation, it guarantees that these quantum trajectories are the paths along which probability flows and the observable results can be exactly computed from the quantum trajectory [15].

The methods to calculate quantum trajectory can be divided into two broad categories [16]. The first one includes those methods to solve S directly from the hydrodynamical equations, Eqs. (2) and (3). Computation is usually quite difficult [17] when evaluating the second-order spatial derivatives. Another group of methods deals with the problem in two steps. Firstly the wave function is obtained by solving the TDSE with a suitable time propagation scheme, then S is derived from wave function. Once S is known, the quantum trajectories are calculated according to Eqs. (4) and (5). The main advantage of the second group of methods is that many robust methods have been developed to solve exactly the TDSE, e.g. split operator method for wavepacket propagation [18], multislice method [19] or Bloch wave method [20] for imaging simulation in electron microscopy.

We employ the split operator method proposed by Feit et al. [18] for numerical solution of the TDSE. The formal solution of TDSE is $\psi(t+dt) = e^{(-i\hat{H}dt/\hbar)} \psi(t)$,

where $\hat{H} = -\frac{\hbar^2}{2m} \nabla^2 + V(\mathbf{r}, t) = \hat{T} + \hat{V}$ is the Hamiltonian.

The split operator method [18], with a third-order accurate formula in time, splits the exponential time propagator $e^{(-i\hat{H}dt)}$ into three parts,

$$e^{-i\hat{H}dt/\hbar} = e^{-i\hat{T}dt/2\hbar} e^{-i\hat{V}dt/\hbar} e^{-i\hat{T}dt/2\hbar} + o((dt)^3).$$

The kinetic energy \hat{T} operator and potential energy \hat{V} operator are diagonal in momentum and configuration space, respectively. So the time evolution operator, $e^{-i\hat{V}dt/\hbar}$, arising from the potential energy, is easily operated in the real space where it means a multiplication and a function evaluation in real space. While the time evolution operator, $e^{-i\hat{T}dt/2\hbar}$, arising from the kinetic energy, is operated in the momentum space where it also means a multiplication and a function evaluation in momentum space. The transformation between the momentum space and the real space can be achieved

effectively by fast Fourier transform (FFT). With the help of the FFT algorithm, this procedure is very efficient and very accurate. This method is unconditionally stable and norm preserving since only unitary operators are involved. Then the quantum trajectories are calculated according to Eqs. (4) and (5) by fourth order Rung-Kutta integration scheme.

In this work, we treat only the electron elastic scattering in solid. In general the difference between the real crystal potential and that of a model crystal composed of isolation atoms is very small [21]. For most of the inorganic crystals, crystal potential can be written as [21] $V(\mathbf{r}) = \sum_n \sum_i \varphi(\mathbf{r} - \mathbf{R}_n - \mathbf{r}_i)$, where n denotes

the n th unit cell of the crystal and i the i th atom in the unit cell. The atomic potential φ can be obtained from inverse Fourier transform of the atomic scattering factor. For a qualitative study of the electron diffraction in crystal, we consider an analytical pseudo potential [22].

$$V(\mathbf{r}) = \sum_i C \frac{1 - \gamma^2}{1 - 2\gamma \cos(\omega r_i) + \gamma^2} \quad (6)$$

where C , ω and γ modulate the value, period, and smoothness of the potential, respectively. An initial incoming plane wave of electrons can be approximated as a linear superposition of Gaussian wave packet, expressed as,

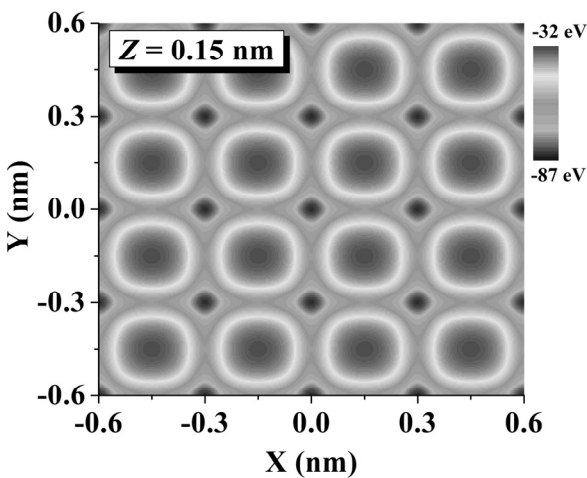


Fig. 1 A cross-section plane of the crystal potential for electron scattering inside a modeled thin film crystal.

$$\psi(x, y, z; t=0) = C \sum_i \exp\left\{-\frac{(x-x_0^i)^2}{2\sigma_1^2} - \frac{(y-y_0^i)^2}{2\sigma_2^2} - \frac{(z-z_0^i)^2}{2\sigma_3^2}\right\} \exp(i\mathbf{k} \cdot \mathbf{r}) \quad (7)$$

where σ is the spatial dispersion, (x_0^i, y_0^i, z_0^i) the central position of the i th wave packet at time $t=0$, C the normalization constant, \mathbf{k} the wave vector and \mathbf{r} the position vector.

3. Results and discussion

We have simulated the elastic scattering of electrons in a modeled thin film crystal, whose potential parameters are: $C = -20$ eV, $\omega = 2\pi / 0.3$ nm⁻¹ and $\gamma = 0.2$. Electrons are incident normal to a crystal surface along z -axis. The lattice constant is taken as 0.3 nm. The modeled thin film crystal, whose thickness is 0.6 nm, consists of three atomic mono-layers. The crystal has periodical cubic structure in $x-y$ plane. Fig. 1 shows crystal potential in a cross-section plane ($x-y$ plane) parallel to the surface. The primary energy E_p is 700 eV, corresponding to a de Broglie wavelength of $\lambda = 0.046$ nm. Initial incoming plane wave is approximated as a linear superposition of 200×200 Gaussian wave packets, uniformly distributed in the $x-y$ plane. The spatial dispersion of each Gaussian wave packet is: $\sigma_x = \sigma_y = 0.06$ nm and $\sigma_z = 0.3$ nm. The resulting plane wave is then launched from $\langle z \rangle = -0.8$ nm (the lower surface is set as $z = 0$). The time step dt is 0.005 a.u. The initial positions of Bohmian particles are chosen according to the probability density function of electron incoming plane wave.

Fig. 2 shows the evolution of electron wave function, by displaying snapshots of the probability density function of electrons scattered by the crystal potential at different times in a plane parallel to surface. We can see that the initial electron plane wave function splits into many diffraction channels. Fig. 2(a) shows the waves inside the solid where the diffraction channels are under formation. After electron wave penetrates the thin film crystal, diffraction is gradually becoming obvious via Talbot effect as shown in Figs. 2(b) and 2(c). In Fig. 2(b) the diffraction peaks represented by the maxima corresponds well with the minima of the periodical crystal potential in Fig. 1. Fig. 2(c) indicates that the diffraction pattern shifts to show opposite maxima and minima with respect to those in Fig. 2(b). This is due to

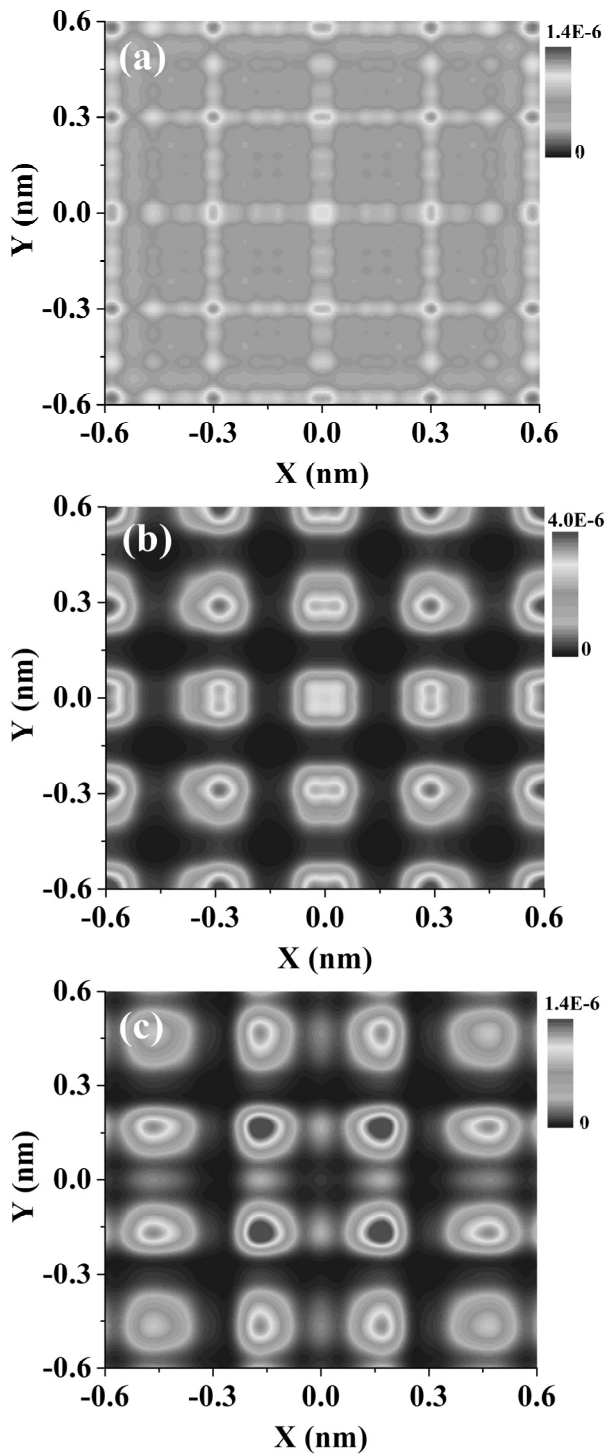


Fig. 2 Probability density function of electrons in $x - y$ plane scattered by crystal potential: (a) $t = 0.06$ fs at $z = 0.24$ nm ; (b) $t = 0.12$ fs at $z = 1.12$ nm ; (c) $t = 0.25$ fs at $z = 2.88$ nm.

the Talbot effect, which is a near-field diffraction effect first observed in 1836 by Talbot [23]. It has important technological application in optics and electron microscopy. Talbot revivals behind crystals have been imaged directly in transmission electron microscopy [24].

In electron diffraction the periodical crystal plays the role of diffraction grating [25].

The time evolution of Bohmian particle trajectories representing electron diffraction is shown in Fig. 3. These particles are initially distributed according to the probability density function of electron incoming plane wave. Fig. 3 (a) shows the assembly of the particles at time $t = 0.12$ fs. It is clear that their spatial distribution agrees with the probability density function at the same time shown in Fig. 2(b). A series of snapshots form an animation for the dynamic process of electron trajectories in diffraction. The result demonstrates that Bohmian quantum trajectory theory can provide an intuitive dynamics of the interaction process of electron and solid, meanwhile preserve the same accuracy of prediction as made by conventional quantum theory. The continuity equation, Eq. (3), guarantees that [26] if initial positions of Bohmian particles are sampled from the probability density function at time $t = 0$, then the configuration of the particles is distributed according to the probability density function at any later time.

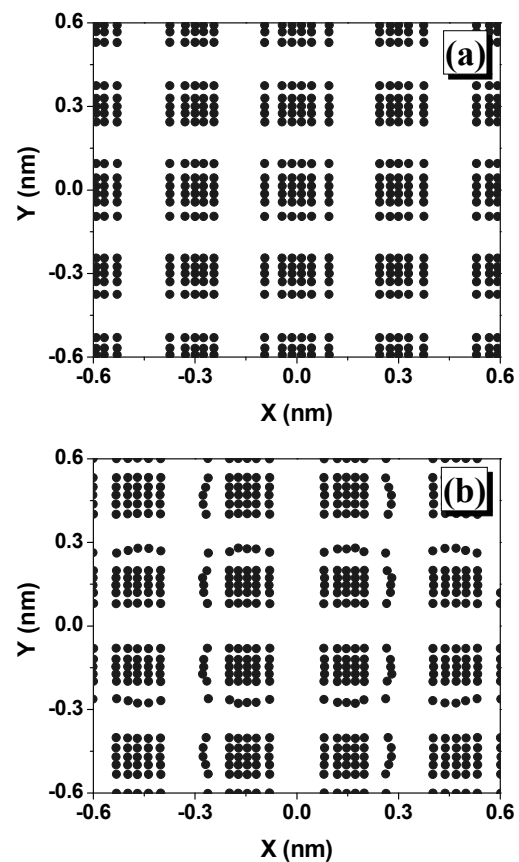


Fig. 3 The assembly of Bohmian particles in $x - y$ plane: (a) $t = 0.12$ fs; (b) $t = 0.25$ fs.

4. Conclusion

Bohmian quantum trajectory theory opens a new way to understand the phenomena of electron-matter interaction. The Bohmian particle trajectories reproduce the electron diffraction pattern very well. Such an example calculation shows its great useful application in future for a theoretical study of electron interaction with solids, surface and nanomaterials to replace the role of classical Monte Carlo electron trajectory method. Once electron inelastic scattering is included via an optical potential [27], the method can be applied to both the techniques of electron microscopy and electron spectroscopy.

5. Acknowledgments

This work is supported by the National Natural Science Foundation of China (Grant Nos. 11074232 and 10874160), “973” project (No. 2011CB932801) and “111” project.

6. References

- [1] M.A. Van Hove, S.Y. Tong, *Surface Crystallography by LEED: Theory, Computation and Structural Results*. Berlin, Springer-Verlag, (1979).
- [2] L. Reimer and H. Kohl, *Transmission Electron Microscopy: Physics of Image Formation*, Springer, Berlin, (2008).
- [3] S. Adam, K. Mukul, P.F. David and L.A. Brent, *Electron Backscatter Diffraction in Materials Science*, New York, Springer, (2009).
- [4] Z.J. Ding, T. Nagatomi, R. Shimizu and K. Goto, *Surf. Sci.* 336, 397 (1995).
- [5] Z.J. Ding, H. M. Li, K. Goto, Y. Z. Jiang and R. Shimizu, *J. Appl. Phys.* 96, 4598 (2004).
- [6] Z.J. Ding, H.M. Li, X.D. Tang and R. Shimizu, *Appl. Phys. A: Mater. Sci. Process.* 78, 585 (2004).
- [7] A. Tonomura, J. Endo, T. Matsuda, T. Kawasaki and H. Ezawa, *Am. J. Phys.* 57, 117 (1989).
- [8] L. de Broglie, *Ann. Phys.* 3, 22 (1925).
- [9] D. Bohm, *Phys. Rev.* 85, 166 (1952).
- [10] D. Bohm, *Phys. Rev.* 85, 180 (1952).
- [11] C. Philippidis, C. Dewdney and B. J. Hiley, *II Nuovo Cimento B* 52, 15 (1979).
- [12] A.S. Sanz, F. Borondo and S. Miret-Artés, *Phys. Rev. B* 61, 7743 (2000).
- [13] A.S. Sanz, F. Borondo and S. Miret-Artés, *Europhys. Lett.* 55, 303 (2001).
- [14] D. Bohm, *Wholeness and the Implicate Order*, London, Routledge and Kegan, (1980).
- [15] X. Oriols, *Phys. Rev. Lett.* 98, 066803 (2007).
- [16] A.S. Sanz, F. Borondo and S. Miret-Artés, *J. Phys.: Condens. Matter.* 14, 6109 (2002).
- [17] R.E. Wyatt, *Quantum Dynamics with Trajectories*, New York, Springer, (2005).
- [18] M.D. Feit, Jr. J.A. Fleck and A.S. Steiger, *J. Comput. Phys.* 47, 412 (1982).
- [19] E.J. Kirkland. *Advanced Computing in Electron Microscopy*. Plenum, New York, 1998.
- [20] J.C.H. Spence and J.M. Zuo. *Electron Microdiffraction*, Plenum, New York, 1992.
- [21] L.M. Peng, *Micron* 30, 625 (1999).
- [22] L. Wille, H. Vershelde and P. Phariseau, *J. Phys. A: Math. Gen.* 16, L771 (1983).
- [23] H.F. Talbot, *Philos. Mag.* 9, 401 (1836).
- [24] J.C.H. Spence, *High-Resolution Electron Microscopy*, Oxford University Press, New York (2003)
- [25] B. J. McMorran and A. D Cronin, *New J. Phys.* 11,033021 (2009).
- [26] D.A. Deckert, D. Dürr and P. Pickl, *J. Phys. Chem. A* 111, 10325 (2007).
- [27] R.G. Zeng and Z.J. Ding, to be submitted.